Passive vibration damping enhancement of piezoelectric shunt damping system using optimization approach [†]

Jin-Young Jeon[*]

Digital Printing Division, Digital Media & Communications Business, Samsung Electronics Co., Ltd., Suwon-City, 443-742, Korea

---

Abstract

Piezoelectric materials can be used for structural damping because of their ability to efficiently transform mechanical energy to electrical energy and vice versa. The electrical energy may be dissipated through a connected load resistance. In this paper, a new optimization technique for the optimal piezoelectric shunt damping system is investigated in order to search for the optimal shunt electrical components of the shunt damping circuit connected to the piezoelectric patch on a vibrating structure for the structural vibration suppression of several modes. The vibration suppression optimization technique is based on the idea of using the piezoelectric shunt damping system, the integrated p-version finite element method (p-version FEM), and the particle swarm optimization algorithm (PSOA). The optimal shunt electrical components for the piezoelectric shunt damping system are then determined by wholly minimizing the objective function, which is defined as the sum of the average vibration velocity over a frequency range of interest. Moreover, the optimization technique is performed by also taking into account the inherent mechanical damping of the controlled structure with the piezoelectric patch. To numerically evaluate the multiple-mode damping capability by the optimal shunting damper, an integrated p-version FEM for the beam with the shunt damping system is modeled and developed by MATLAB. Finally, the structural damping performance of the optimal shunt damping system is demonstrated numerically and experimentally with respect to the beam. The simulated result shows a good agreement with that of the experimental result.

Keywords: Piezoelectric shunt damping system; P-version FEM; Mobility; Passive vibration damping enhancement

---

1. Introduction

Structural damping is an important way of reducing vibration, noise and mechanical fatigue. The use of high loss factor viscoelastic materials is one of the most common passive damping methods[1]. The damping effects of a viscoelastic material are located in the glass transition region, where a loss peak occurs. The width of the transition region determines the temperature or frequency range of the damping performance, and the height of the transition region determines the damping effectiveness. Thus it is desir-

able for viscoelastic materials to have a broad, high loss peak in damping applications. However, this requirement is difficult because broadening of the loss peak in viscoelastic materials usually results in a decrease of the peak height and vice versa. This trade-off in width and height limits further development of viscoelastic materials for damping applications.

Piezoelectric materials have been introduced as passive damping materials to overcome this trade-off in the width and height limits of viscoelastic materials. Piezoelectric materials can be used for producing the structural damping because of their unique ability to efficiently transform mechanical energy into electrical energy and vice versa, as shown in Fig. 1.

The passive shunt damping systems for reducing structural vibration of a vibrating structure have been
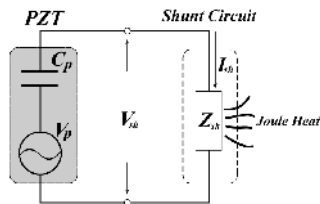
Fig. 1. Equivalent electrical model of a PZT.

studied by some researchers[2-6]. Forward[2] experimentally demonstrated the use of resistive and inductive-resistive resonant piezoelectric shunt circuits to provide damping for structures containing piezoelectric materials. Hagood and von Flotow[3] later presented an analytical model for resistive and inductive-resistive shunt dampened systems. They optimally tuned an electrical resonance of the shunting circuit to structural resonances in a manner analogous to a mechanical vibration absorber for a selected mode. Wu[4] proposed a passive piezoelectric shunting technique using a parallel resistor and inductor circuit connected to two external terminals of a piezoelectric element. He performed the theoretical analysis employing a cantilever beam structure and derived the general equations of displacement, optimum inductance for tuning and optimum resistance for vibration reduction and damping. Edberg et al.[5] experimentally demonstrated that a multi-mode shunt could suppress more than one eigenmode of the structure using a single piezoelectric patch. Hollkamp[6] expanded the theory of piezoelectric shunting for a single mode so that a single piezoelectric material can be used to suppress two modes by optimally designing the shunting parameters. Optimal values for the shunt inductance and resistance were based on the analogy with the damped vibration absorber.

However, all the previously cited papers did not take into account the inherent mechanical damping of the controlled structure and, to the author's knowledge, no formulae for the optimal values of the shunt circuit components considering the inherent mechanical damping have been developed in the literature. Also, in modeling piezoelectric structures with shunt circuits, the conventional mechanical impedance model has been used.

In this paper, a new optimization technique for the optimal piezoelectric shunt damping system is proposed in order to search for the optimal shunt electrical components of the shunt damping circuit connected to the piezoelectric patch on a vibrating struc-

ture for the structural vibration suppression of several modes. The optimization technique is based on the idea of using the piezoelectric shunt damping system, the integrated p-version finite element method (p-version FEM), and the particle swarm optimization algorithm (PSOA)[7].

The optimal shunt electrical components for the piezoelectric shunt damping system are then determined by minimizing the objective function, which is defined as the sum of the average vibration velocity over a frequency range of interest. Moreover, optimization is performed by also taking into account the inherent mechanical damping of the controlled structure with the piezoelectric patch, which turns out to influence the optimal values of the electrical parameters. To numerically evaluate the multiple-mode damping capability by the optimal shunting damper, the integrated p-version FEM for the beam with the shunt damping system is modeled and developed by MATLAB. The analytical model of the piezoelectric patch shunted with the multiple-mode damping circuit is derived from the p-version FEM. Finally, to confirm the validity and effectiveness of the optimization approach for the piezoelectric shunt damper based on the PSOA, the structural damping performance of the optimal shunt damping system is demonstrated numerically and experimentally with respect to the beam. The simulated result shows a good agreement with that of the experimental result.

2. General theory and modeling of the piezoelectric shunt damping system

The electromechanical coupling analysis of the global system with the shunted piezoelectric is described in this section. A three-dimensional finite element code by using p-version FEM is developed in order to analyze the electromechanical model of piezoelectric materials by using MATLAB. The outline of the implementation of PSOA in the optimization approach for the piezoelectric shunt damping system is described.

2.1 Piezoelectric analysis by using p-version FEM

Recently, there has been a growing interest in the simulation of the piezoelectric mechanisms as well as the piezoelectric passive damping system by means of resonant shunt damping circuits.

In the present study, p-version FEM using an eight-node, 32 degree-of-freedom brick element together

with the shape functions of incompatible modes is developed for the piezoelectric analysis of a simple cantilever beam with the bonded piezoelectric material, as depicted in Fig. 4.

In general, the electromechanical constitutive equations of piezoelectric material behavior can be written according to IEEE Standard[8] as:

$$\begin{Bmatrix} T \\ D \end{Bmatrix} = \begin{bmatrix} c^E & -e \\ e^t & \varepsilon^S \end{bmatrix} \begin{Bmatrix} S \\ E \end{Bmatrix} \tag{1}$$

where T is the stress vector (force/area), D is the electric displacement vector (charge/area), S is the strain vector, E is the electric field vector (volts/meter), c^E is the elasticity stiffness matrix evaluated at constant electric field (e.g., short circuit ($E = 0$)), e is the piezoelectric stress matrix, ε^S is the dielectric matrix evaluated at a constant mechanical strain (e.g., clamped ($S = 0$)), and t denotes matrix transpose. After the application of Hamilton's principle and finite element discretization for coupled electromechanical systems, the coupled finite element matrix equations for each element model can be derived in terms of extended nodal displacements as:

$$\begin{bmatrix} M & 0 \\ 0 & 0 \end{bmatrix} \begin{Bmatrix} \ddot{w} \\ \ddot{v} \end{Bmatrix} + \begin{bmatrix} C & 0 \\ 0 & 0 \end{bmatrix} \begin{Bmatrix} \dot{w} \\ \dot{v} \end{Bmatrix} + \begin{bmatrix} K & \Theta \\ \Theta^t & -C_P \end{bmatrix} \begin{Bmatrix} w \\ v \end{Bmatrix} = \begin{Bmatrix} F \\ q \end{Bmatrix} \tag{2}$$

where $[M]$, $[C]$, $[K]$ and $[\Theta]$ represent the global mass matrix, the global damping matrix, the global stiffness matrix and the electromechanical coupling matrix of the host structure and the piezoelectric material, respectively, $[C_P]$ is the inherent piezoelectric capacitance matrix, $\{F\}$ is the applied mechanical force vector, $\{q\}$ is the electric charge vector, $\{w\}$ is the generalized mechanical coordinate and $\{v\}$ is the generalized electrical coordinate, which is the physical voltage at the piezoelectric electrodes. The damping matrix $[C]$ is assumed to be a proportional viscous damping in this study.

From Eq. (2), the equation of motion of the piezoelectrically coupled electromechanical system can be rewritten by two sets of coupled equations as follows:

$$[M]\{\ddot{w}\} + [C]\{\dot{w}\} + [K]\{w\} + [\Theta]\{v\} = \{F\}$$
$$[\Theta]^t\{w\} - [C_p]\{v\} = \{q\}. \tag{3}$$

The first set describes the equilibrium condition of mechanical forces and the second set is an electrodynamics condition of electric potential. These two sets of equations can be employed to derive the piezoelectric passive damping force by means of shunt damping circuits connected to the piezoelectric electrodes. When a piezoelectric patch is shunted by an impedance Z_{sh} as shown in Fig.1, the shunt damping voltage across the shunt damping network can be represented by the current-voltage relationship in the Laplace domain as:

$$V_{sh}(s) = Z_{sh}(s) \cdot I_{sh}(s) \tag{4}$$

where $V_{sh}(s)$ is the voltage across the impedance and $I_{sh}(s)$ is the current flowing through the impedance. The current can be also obtained by differentiating the second set of Eq. (3). By substituting it into Eq. (4),

$$V_{sh}(s) = Z_{sh}(s) \cdot \dot{q}(s)$$
$$= Z_{sh}(s) \cdot ([\Theta]^t\{w\}s - [C_p]V_{sh}(s)s) \tag{5}$$

and rearranging, the shunt voltage equation is derived as follows:

$$V_{sh}(s) = \frac{Z_{sh}(s)[\Theta]^t\{w\}s}{1 + Z_{sh}(s)[C_p]s} \tag{6}$$

where s is the Laplace operator.

Substituting Eq. (6) into the first set of Eq. (3), the governing equation of the shunted piezoelectric can be derived by considering the additional passive piezoelectric damping force as follows:

$$[M]\{\ddot{w}\} + ([C] + Z_{total}[\Theta][\Theta]^t)\{\dot{w}\} + [K]\{w\} = \{F\} \tag{7}$$

where the total electrical impedance of the shunted piezoelectric Z_{total} includes the inherent capacitance of the piezoelectric and can be expressed by

$$Z_{total} = \frac{Z_{sh}}{1 + Z_{sh}[C_p]s} \tag{8}$$

Eq. (7) is transformed into the modal domain by using the following modal coordinate transformation:

$$\{w\} = [\Phi]\{\xi\} \tag{9}$$

where $[\Phi]$ is a truncated eigenvector matrix of the system and $\{\xi\}$ is a modal coordinate vector. Substituting Eq. (9) and pre-multiplying the transposed matrix of $[\Phi]$ into Eq. (7), and then transforming it into frequency domain, the uncoupled equations of motion of the harmonic forced vibration in the modal domain are obtained as follows:

$$-\omega^2[m]\{\xi\}+j\omega([c]+Z_{total}[\theta])\{\xi\}+[k]\{\xi\}=\{f\} \quad (10)$$

$$\{\xi\}=\left(-\omega^2[m]+j\omega([c]+Z_{total}[\theta])+[k]\right)^{-1}\{f\} \quad (11)$$

where $[m], [c], [k]$ and $[\theta]=[\Phi]^t[\Theta][\Theta]^t[\Phi]$ are the modal mass, the modal damping, the modal stiffness and the modal electromechanical coupling, respectively, $\{f\}$ is the modal excitation force, j is $\sqrt{-1}$, and ω is an angular frequency of vibration.

The velocity transfer function (Mobility) for a structure with the piezoelectric shunt damping system can be expressed in the modal coordinates as follows:

$$D(\omega)=\frac{\dot{W}_j(\omega)}{F_i}$$
$$=\sum_{r=1}^{N}\frac{\phi_{ri}\cdot\phi_{rj}}{m_r j\omega+(c_r+Z_{total}\cdot\theta_r)+k_r/(j\omega)} \quad (12)$$

where ϕ_{ri} and ϕ_{rj} are the elements i and j, respectively, of the r th eigenvector matrix.

2.2 Particle swarm optimization

Particle swarm optimization (PSO), which was proposed by Kennedy and Eberhart[7], originated from a simulation algorithm for simplified social behaviors of organisms, such as bird flocking and fish schooling, developed by zoologists. It comprises a very simple concept that requires only primitive mathematical operators so that it is computationally inexpensive in terms of both computer memory and speed.

Let q be the number of the PSO population. For particle d ($d=1,2,\ldots\ldots.q$), Kennedy and Eberhart initially proposed that, for simulating the social behavior of birds, the position x^d in PSO be updated as

$$x_{k+1}^d = x_k^d + v_{k+1}^d \quad (13)$$

and the velocity v^d be updated as:

$$v_{k+1}^d = v_k^d + c_1 r_1(p_k^d - x_k^d) + c_2 r_2(p_k^g - x_k^d) \quad (14)$$

where the subscript k is a time increment counter, r_1 and r_2 are stochastic factors in the range $[0,1]$, c_1 and c_2 are constants, called acceleration coefficients, that are recommended by the developers and that control the maximum step size the particle can perform, p_k^d represents the best ever position (i.e., the best position of the d th particle that minimizes the objective function until the k th optimization process) of particle d at time k, and p_k^g represents the global best ever position (i.e., the global best position among all particles that minimizes the objective function until the k th optimization process) in the swarm until time k.

Furthermore, by adding a new inertia weight λ into Eq. (14), a new modified formulation of PSO was proposed by Eberhart et al.[9] as follows:

$$v_{k+1}^d = \lambda v_k^d + c_1 r_1(p_k^d - x_k^d) + c_2 r_2(p_k^g - x_k^d) \quad (15)$$

They proposed $0.8<\lambda<1.4$ as the appropriate range of λ. The inertia weight, which is a user-specified parameter, is used to control the impact of the previous historical values of the particle velocities on the current velocity. A larger inertia weight facilitates flying toward global exploration, searching a new area, while a smaller inertia weight tends to facilitate fine-tuning of the current search area. Appropriate selection of the inertia weight and acceleration coefficients can provide a balance between global and local exploration abilities, and thus, on average, the optimal solution can be found in a fewer iterations. Eq. (14) is employed in order to obtain the new velocity of the particle according to its previous velocity and the distance of its current position from both its own best historical position and its neighbors' best position. Then, the particle d in PSO moves to a new position according to Eq. (13).

2.3 PSO algorithm for optimal piezoelectric shunt damping system

The main purpose of the optimization technique is to search for the optimal shunt components of the piezoelectric shunt damping system in order to efficiently damp and attenuate the peak vibration amplitudes from a vibrating structure. Then, in tuning the optimal parameter for the piezoelectric shunt damping circuit, the average velocity transfer function B_w

over a frequency range of interest, which is derived from the velocity transfer function D in Eq. (12), is adopted as the objective function to be minimized in the optimization process. Moreover, the optimization approach is performed by also taking into account the inherent mechanical damping of the controlled structure.

The average velocity transfer function and the objective function are expressed by Eqs (16a) and (16b), respectively.

$$B_w = \frac{1}{N_f} \sum_{i=1}^{N_f} D(\omega_i) \tag{16a}$$

Minimize B_w (16b)

The feasible design area of the variables must be bounded in practice. Then, the upper and lower bounds of the design variables are expressed as:

$$\underline{R}_i \le R_i \le \overline{R}_i \quad (i = 1 \sim 2) \tag{17}$$

where $\underline{R}_i$ and $\overline{R}_i$ are the lower and the upper boundary of piezoelectric shunt resistance (R_i) number i, respectively.

3. Passive vibration damping enhancement using piezoelectric shunt damping device

Two types of broad categories for the combination of the shunt resonant damping circuit which mainly consists of a series R-L and a parallel R-L are considered next.

Firstly, single-mode R-L shunt damping circuit[2-4] can be used to reduce and damp only one structural vibration mode. Single-mode shunt damping experiments are performed in order to verify the validity of the simulation method based on p-version FEM model.

Secondly, there are several types of multiple-mode shunt damping circuits[6, 10] to damp several modes simultaneously. The piezoelectric shunt damping circuit chosen in the present paper is a simplified series-parallel shunt circuit[10] for attenuating multiple-mode from a cantilever beam using a piezoelectric patch only. Although other shunting concepts exist, these shunt circuits were adopted because it had successfully been used for other applications.

3.1 Series R-L shunt circuit for single-mode

First, optimum resistor and inductor values for a series configuration can be obtained by using the method outlined by Wu[4]. The optimal tuning ratio δ_s^* and the optimal damping ratio r_s^* for a series shunt circuit can be written by:

$$\delta_s^* = \sqrt{1 - K_{31}^2/2}, \quad r_s^* = \frac{1}{\sqrt{2} K_{31}}. \tag{18}$$

The optimum series inductance L_s^*, and the optimum series shunt resistance R_s^*, are in turn:

$$L_s^* = \frac{1}{C_p^S (\omega_s \delta_s^*)^2}, \quad R_s^* = \frac{r_s^*}{\omega_s C_p^S}. \tag{19}$$

Here, the PZT capacitance at constant strain C_p^S, is obtained from:

$$C_p^S = C_p^T (1 - k_{31}^2) \tag{20}$$

This capacitance is dependent upon the electromechanical coupling coefficient k_{31}, provided by the PZT manufacturer, and C_p^T is the PZT capacitance at constant stress. If the PZT is already bonded to the host structure, the measured capacitance is close to C_p^S.

The generalized electromechanical coupling coefficient for a transverse mode 31 can be obtained from the resonance frequency change with respect to the electric boundary conditions:

$$K_{31} = \sqrt{(\omega_o^2 - \omega_s^2)/\omega_s^2} \tag{21}$$

where ω_o and ω_s are the natural frequencies of the structural vibration mode, when the two external terminals of the PZT patch are, respectively, on an open-
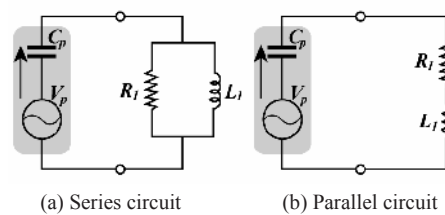

(a) Series circuit   (b) Parallel circuit

Fig. 2. Single-mode shunt damping circuits.

circuit and short-circuited.

The electrical impedance expression of the series shunt circuit shown in Fig. 2(a) is:

$$Z_{sh}^s = \frac{R_s^* L_s^* s}{L_s^* s + R_s^*}, \tag{22}$$

and substituting Eq. (22) into Eq. (8), the total electrical impedance expression of the shunted piezoelectric is:

$$Z_{total}^s = \frac{R_s^* L_s^* s}{R_s^* L_s^* C_p s^2 + L_s^* s + R_s^*}. \tag{23}$$

Also, substituting Eq. (23) into Eq. (12), the velocity transfer function of a structure with the series resistor-inductor shunt circuit can be derived.

3.2 Parallel R-L shunt circuit for single-mode

Next, optimum resistor and inductor values for the parallel shunt circuit can be also calculated following the procedures first derived by Hagood and von Flotow[3]. The optimal tuning ratio δ_p^* and the optimal damping ratio r_p^* for a series shunt circuit can be written as:

$$\delta_p^* = \sqrt{1 + K_{31}^2}, \quad r_p^* = \sqrt{2} \frac{K_{31}}{1 + K_{31}^2}. \tag{24}$$

and then the optimum parallel inductance L_p^*, and the optimum parallel shunt resistance R_p^*, are in turn:

$$L_p^* = \frac{1}{C_p^S (\omega_s \delta_p^*)^2}, \quad R_p^* = \frac{r_p^*}{\omega_s C_p^S}. \tag{25}$$

As shown in Fig. 2(b), the electrical impedance of the parallel shunt circuit is given by:

$$Z_{sh}^p = L_p^* s + R_p^* \tag{26}$$

Substituting Eq. (26) into Eq. (8), the total electrical impedance of the shunted piezoelectric is obtained from

$$Z_{total}^p = \frac{L_p^* s + R_p^*}{L_p^* C_p s^2 + R_p^* C_p s + 1}. \tag{27}$$

Also, the transfer function of a global structure with the parallel resistor-inductor shunt circuit can be calculated by substituting Eq. (27) into Eq. (12).

3.3 Multiple-mode resonant shunt damping circuit

A modified current blocking circuit[10] was applied to control several modes at the target resonance frequencies. Although the modified current blocking circuit is similar in nature to the traditional current blocking circuit proposed by Wu[11], the former contains fewer electrical components than the latter, and may be suitable for the application of multiple-mode shunt damping circuit. The current blocking circuits in each branch network are connected in parallel to the shunt damping circuits to reduce the structural modes at the specific target frequencies. The series-parallel multimode impedance circuit consists of two sub-networks: a parallel current blocking circuit $C_i - \hat{L}_i$, and a parallel single-mode shunt damping network $\widetilde{L}_i - R_i$. The parallel current blocking circuits are tuned to the target resonance frequencies ω_i, and then appear to be approximately open circuit, infinite impedance at the resonance frequencies. That is, the current blocking circuit in each branch network has an extremely large electrical impedance at a specific structural resonance frequency ω_i, while has a low impedance at all other specific resonances except its own resonance frequency.

Consequently, a voltage generated from the electrodes of the PZT piezoelectric transducer results in a current that flows freely through the detuned low electrical impedance current blocking networks. The parallel $\widetilde{L}_i - R_i$ shunt damping circuit connected in parallel to the capacitor of the PZT piezoelectric

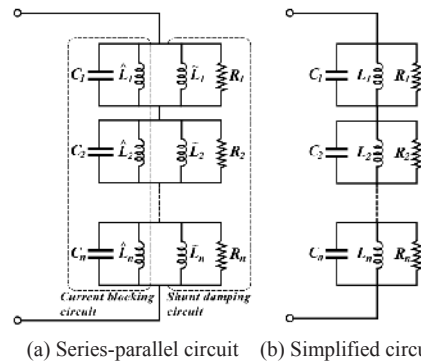(a) Series-parallel circuit   (b) Simplified circuit

Fig. 3. Simplified series-parallel shunt circuit for multiple-mode.

transducer can be independently tuned to each target resonance frequency. As described in Eq. (28), the optimum inductors for the current blocking and shunt damping circuit can be calculated from

$$\hat{L}_i = \frac{1}{\omega_i^2 C_i}, \qquad \tilde{L}_i = \frac{1}{\omega_i^2 C_p} \qquad (28)$$

where ω_i is the i th target resonance frequency, C_i is an arbitrary capacitance, and C_p is the inherent capacitance of the PZT piezoelectric transducer.

More simply, as shown in Fig. 3, the series-parallel circuit (Fig. 3(a)) can be transformed into the simplified circuit (Fig.3 (b)). The electrical impedance of the simplified series-parallel shunt damping circuit can be calculated as follows:

$$Z_{sh}(s) = \sum_{i=1}^{n} \frac{1}{C_i s + \frac{1}{R_i} + \frac{1}{L_i s}} \qquad (29)$$

where L_i is the combined inductance resulting from $\hat{L}_i$ and $\tilde{L}_i$, and n is the number of the target modes.

Substituting Eq. (29) into Eq. (8), the total electrical impedance of the simplified series-parallel shunt circuit can easily be obtained. Combining Eq. (8) into Eq. (12), the simulation for the multiple-mode shunt damping can be carried out.

4. Vibration suppression of a cantilever beam

4.1 Experimental configurations

Multiple-mode shunt damping experiments were performed to verify the validity and effectiveness of the proposed optimization approach based on PSOA, and of the passive damping performance of the piezoelectric shunt damping system on the aluminum cantilever beam. This section will show the comparisons between the simulation and experiment performed on the single-mode and the multiple-mode shunt damping circuit.

The cantilever beam has dimensions of $0.2 \times 0.06\,\text{m}$ with thickness $0.0015\,\text{m}$. The material properties of the beam are a Young's modulus of $64\,\text{GPa}$, a Poisson's ratio of 0.27, and density of $2730\,\text{kg}/\text{m}^3$. The beam has a clamped boundary condition at its base ($x = 0$). A PZT piezoelectric patch (Fuji Ceramics, PZT C-82) having the size of

Table 1. Properties of the PZT C-82.

Properties	Values
Charge constant, d_{31}	$-210 * 10^{-12}\,\text{m}/\text{V}$
Coupling coefficient, k_{31}	0.37
Young's modulus, Y_{11}	62 Gpa
Poisson ratio, v	0.34
Dielectric constant, ε_{33}	3650
Density, ρ	$7500\,\text{kg}/\text{m}^3$
Curie temperature	$195\,^\circ C$
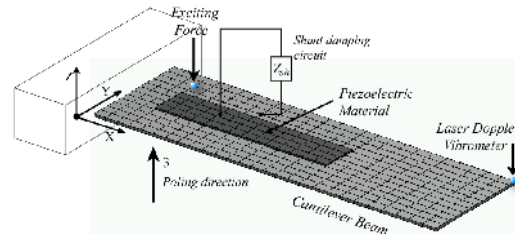
Fig. 4. A cantilever beam with the shunted piezoelectric patch.

$0.1 \times 0.02\,\text{m}$ with thickness 0.001m is bonded on the upper surface of the root of the cantilever beam using a very thin layer of epoxy. The PZT patch is located 0.02 m away from the base of the beam. The physical properties of the PZT piezoelectric material are presented in Table 1. The capacitance of the PZT C-82 bonded to the beam is measured by the LCR impedance analyzer. The PZT piezoelectric patch is poled through its thickness in the positive z direction so that it is operating in transverse mode (d_{31}). The shunt damping circuit is connected in parallel to the electrodes of the PZT piezoelectric patch as shown in Fig. 4. The negative electrode connected to the shunt damping circuit is grounded to the beam.

The beam is excited by an impact hammer at a point (0.02,0.05,0.0015), and the velocity in time domain and the velocity transfer function are measured using a laser Doppler vibrometer at a point (0.2,0.06,0.0015) and a FFT analyzer.

4.2 Single-mode shunt damping

The series R-L and the parallel R-L single-mode shunt circuit were both used experimentally to damp the 1st bending mode of the cantilever beam. To confirm the validity of the simulation method based on p-version FEM, the experimental results are also compared with the simulated results of the beam obtained analytically from the p-version FEM analysis. In order to design the optimal shunt tuning inductor and resistor to be used in the shunt circuit

for single-mode by using Eq. (19) and Eq. (25) are then determined from the experiment as described below:

1. Obtain the natural frequencies ($f_o = 35.8$ Hz, $f_s = 35.4$ Hz) when the piezoelectric patch is on an open circuit and then shorted.

2. Calculate the generalized transverse electro-mechanical coupling coefficient ($K_{31} = 0.1508$), and the capacitance ($C_p^T = 67.2$ nF) of the piezoelectric patch at constant stress.

The theoretical optimal shunting components obtained with the optimum tuning procedures, as shown in the left column of Table 2, are based on the retuned optimal shunt electrical components of the actual experiment in the right column of Table 2. To reach the optimum vibration reduction, this would require several iterative operations between the L and R, which is a tedious and time-consuming operation. The optimal shunt electrical parameters used in the simulation are also listed in the middle column of Table 2. Then, since the inductance value of the shunt circuits is too large to be implemented using a coil, a synthetic inductor[12, 13] with two Op-Amps is used. The synthetic inductor is chosen for its convenience, light-weight, and can easily adjust the inductance value by using a variable resistor ($\overline{R}_2$) as described in Fig. 5.

Table 2. Optimal electrical components for a series R-L and a parallel R-L shunt damping circuit.

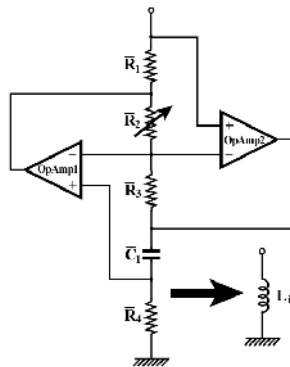| Circuit Type	Simulation		Experiment	
	R	L	R	L
Series	359.9 KΩ	351.4 H	341.5 KΩ	351.5 H
Parallel	16.3 KΩ	339.8 H	15.3 KΩ	340.6 H

Fig. 5. Synthetic inductor.

However, it requires an external power source, and always has several resistive components proportional to the inductance, which is not desirable for designing the optimal resistance in the shunt circuit. Therefore, the actual resistance value of the shunt damping circuit may have some effect due to the resistance associated with the synthetic inductor as describe in Table 2.
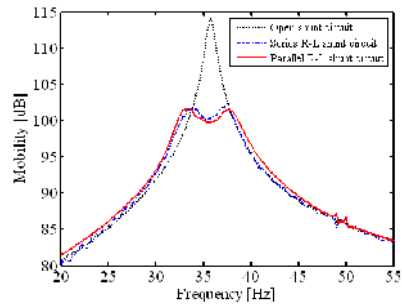
(a) Experimental result
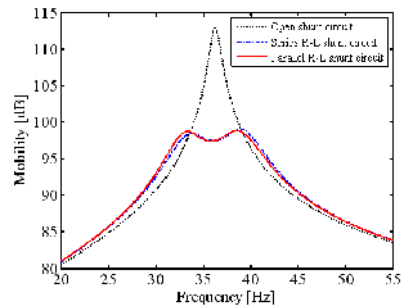
(b) Simulated result

Fig. 6. Comparison of the FRFs for the cantilever beam with a single-mode shunt damping circuit (dot-dashed line: series R-L shunt circuit, solid line: parallel R-L shunt circuit).
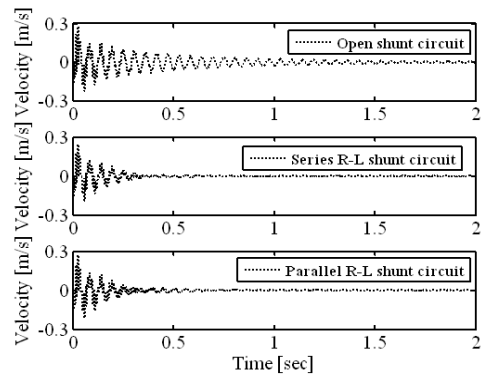

Fig. 7. Experimental time domain responses for the cantilever beam using a single-mode shunt damping circuit.

Fig. 6(a) shows the experimental results performed by using the series R-L shunt circuit and the parallel R-L shunt circuit wired to the electrodes of the piezoelectric patch bonded on the beam. The experimental damping performances with the shunted piezoelectric patch can be further observed by comparing its time response to that of the system with the piezoelectric patch on an open circuit, as shown in Fig. 7. For the 1st bending mode, a 14.1 dB of peak reduction was successfully achieved using the series and the parallel shunt circuits, respectively. The simulation results shown in Fig. 6(b) exhibit a peak amplitude of the first mode reduced by 15.5 dB. Thus, a good agreement was observed between simulation and experimental results. From the cantilever beam example it can be concluded that the p-version FEM model developed in this study can be applied to the piezoelectric shunt damping system.

4.3 Multiple-mode shunt damping

Using the simplified series-parallel structure described in section 3.3, a multiple-mode shunt damping experiment was also performed to damp the first and second bending modes of the cantilever beam. A single PZT piezoelectric patch only, which has the same material properties used in the previous section, was used to reduce two structural resonant modes of the beam simultaneously.

The capacitance values, C_1 and C_2 in the shunt circuit can be arbitrarily chosen, and then the optimum inductance values can be easily calculated from Eq. (28).

An optimization approach based on the PSOA is proposed in order to search for the optimal shunt resistance R_i. The optimization technique was performed to search for the optimal parameter for wholly minimizing the amplitude of the average velocity transfer function over the frequency band of interest. Moreover, the optimization technique was performed by also taking into account the inherent mechanical damping of the controlled structure with the piezoelectric patch. A summary of the components in the simplified series-parallel shunt circuit is provided in Table 3.

The experimental result in Fig. 8(a) shows that the damping performance of the simplified series-parallel shunt circuit can successfully work for the vibration suppression of several structural modes of the beam. The peak reductions of the 1st and 2nd bending modes

Table 3. Component values of the simplified series-parallel circuit for the beam.

Circuit Components	Experimental Values	Simulated Values
C_1	100 nF	100 nF
C_2	200 nF	200 nF
L_1	135.5 H	135.5 H
L_2	2.81 H	2.74 H
R_1	202.1 KΩ	213.3 KΩ
R_2	18.10 KΩ	19.51 KΩ
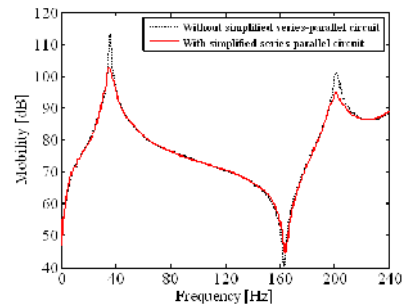
(a) Experimental result
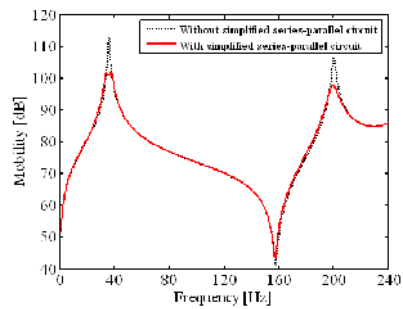
(b) Simulated result

Fig. 8. Comparison of the FRFs for the cantilever beam with the simplified series-parallel shunt damping circuit.
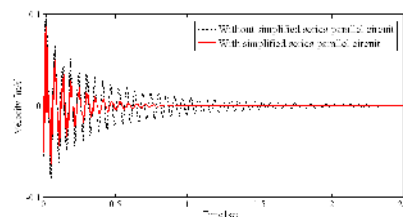

Fig. 9. Experimental time domain responses for the cantilever beam using the simplified series-parallel shunt damping circuit.

were experimentally reduced by 10 dB and 6.2 dB, respectively.

The simulated result calculated by using the analytical model of the developed p-version FEM shown in Fig. 8(b) presents a peak amplitude reduction of the first and second modes of 11 dB and 8.2 dB, respectively. The simulated result shows a good agreement with the experimental result. Although the damping performance of the experimental result was somewhat poorer than that of the simulated result, the author can assume that it was due to the mutual interference between the resistances in the simplified series-parallel shunt circuit and the resistances in the synthetic inductor.

Furthermore, the velocity transfer function at a point (0.2,0.6,0.0015) in the experimental time domain was measured (Fig. 9). The impulse velocity transfer function in time domain shows clearly that the piezoelectric shunt damping system can sufficiently conduct the damping performance in the realistic vibration environment.

5. Conclusions

A new optimization technique for an optimal piezoelectric shunt damping system was investigated in order to search for the optimal shunt electrical components of the simplified series-parallel shunt circuit connected to the piezoelectric patch on a cantilever beam. The passive vibration suppression optimization technique was based on the idea of using the piezoelectric shunt damping system, the integrated p-version finite element method (p-version FEM), and the particle swarm optimization algorithm (PSOA). The optimal shunt electrical components for the piezoelectric shunt damping system were then determined by wholly minimizing the objective function, which is defined as the sum of the average vibration velocity over a frequency range of interest. Moreover, the optimization technique was performed by also taking into account the inherent mechanical damping of the controlled structure with the piezoelectric patch.

Using the simplified series-parallel structure, the multiple-mode shunt damping experiment was also performed to damp the first and second bending modes of the cantilever beam.

To numerically evaluate the multiple-mode damping capability by the optimal shunting damper, the integrated p-version FEM for the cantilever beam with the shunt damping system was modeled and developed by MATLAB.

Finally, the structural damping performance of the optimal shunt damping system was demonstrated numerically and experimentally with respect to the cantilever beam. The simulated result demonstrated a good agreement with that of the experimental result. Although the damping performance of the experimental result was somewhat poorer than that of the simulated result, the author can assume that it was due to the mutual interference between the resistances in the simplified series-parallel shunt circuit and the resistances in the synthetic inductor.

References

[1] A. D. Nashif, D. I. Jones and J. P. Henderson, Vibration Damping, New York : *John Wiley*, (1985).

[2] R. L. Forward, Electronic Damping of Vibrations in Optical Structures, *Appl. Opt.*, 18 (5) (1979) 690-697.

[3] N. W. Hagood and A. Von Flotow, Damping of Structural Vibrations with Piezoelectric Materials and Passive Electrical Networks, *J. Sound Vib.*, 146 (2) (1991) 243-268.

[4] S. Y. Wu, Piezoelectric Shunts with a Parallel R-L Circuit for Structural Damping and Vibration Control, *Proc. SPIE Smart Structures and Materials, Passive Damping and Isolation,* 2720 (1996) 259-269.

[5] D. L. Edberg, A. S. Bicos and J. S. Fechter, On Piezoelectric Energy Conversion for Electronic Passive Damping Enhancement, *Proceedings of Damping*, (1991) paper GBA-1.

[6] J. J. Hollkamp, Multimodal Passive Vibration Suppression with Piezoelectric Materials and Resonant Shunts, *J. Intell. Mater. Syst. Struct.*, 5 (1994) 49-57.

[7] J. Kennedy and R. Eberhart, Particle swarm optimization, *Proc. IEEE Int. Conf. On Neural Networks*, (1996) 1942-1948.

[8] IEEE Standard on Piezoelectric, ANSI/IEEE Standard, (1987) 176.

[9] R. Eberhart and Y. Shi, Comparison between genetic algorithms and particle swarm optimization, *7-th Annual Conf. On Evolutionary Programming*, (1998) 611-616.

[10] A. J. Fleming, S. Behrens and S. O. R. Moheimani, Reducing the Inductance Requirements of Piezoelectric Shunt Damping Systems, *Smart Mater. Struct.*, 12 (2003) 57-64.

[11] S. Y. Wu, Method for Multiple Mode Shunt Damping of Structural Vibration Using a Single PZT Transducer, *Proc. SPIE Smart Structures and Ma-*

terials, Smart Structures and Intelligent Systems, 3327 (1998) 159-168.

[12] R. H. S. Riordan, Simulated Inductor Using Differential Amplifier, *Electron. Lett.*, 3 (1967) 50-51.

[13] W. K. Chen, Passive and Active Filters, *John Wiley & Sons, Inc.*, (1986).

Jin-Young Jeon received his Ph.D. degree in Mechanical and Aerospace Engineering from Tokyo Institute of Technology in 2005. Dr. Jeon is currently a senior engineer at Digital Printing Division, Digital Media & Communications Business at Samsung Electronics Co., Ltd., Korea. His research interests are the areas of structural-acoustic optimization, sound quality, motion quality, and vibration control.